



Shear wave splitting beneath the central Tien Shan and tectonic implications

Aibing Li¹ and Chizheng Chen¹

Received 28 July 2006; revised 23 September 2006; accepted 4 October 2006; published 17 November 2006.

[1] Shear-wave splitting analyses were performed at 30 seismic stations in the central Tien Shan and its vicinity. Fast orientation at most of the stations on the Tien Shan range is ENE-WSW, parallel to the strike of the Tien Shan. It largely reflects a coherent deformation of the lithosphere in response to the NS shortening. Anisotropy with NNE-SSW fast axes is observed within adjacent basins, around the Issyk Kul and near the northwestern Tarim, where the lithosphere is presumably strong, less deformed. The NNE-SSW orientation, which coincides with the surface velocity of the central Tien Shan, can be best explained by shear between the lithosphere and asthenosphere on a regional scale rather than small-scale convection as proposed in previous studies. The dextral Talasso-Fergana fault seems to have little effect on anisotropy at its nearby stations, suggesting this fault is probably confined to the shallow part of the lithosphere. **Citation:** Li, A., and C. Chen (2006), Shear wave splitting beneath the central Tien Shan and tectonic implications, *Geophys. Res. Lett.*, 33, L22303, doi:10.1029/2006GL027717.

1. Introduction

[2] The Tien Shan is the most active intraplate mountain range on the earth. It extends ~2500 km in a roughly EW direction and is bounded by the Tarim block, a Proterozoic terrain to the south, and the Kazakh shield to the north. The central Tien Shan consists of southern, middle, and northern terrains that are divided by two Paleozoic sutures [Windley *et al.*, 1990]. The Talasso-Fergana fault, a dextral strike slip fault, separates the central and western parts of the Tien Shan (Figure 1). Deformation in the Tien Shan has accelerated in the past 20–30 Myr as a consequence of the India-Asia collision [Yin *et al.*, 1998]. GPS measurements and earthquake focal mechanism studies reveal that the Tien Shan is undergoing significant shortening in the NS direction at a rate of ~20 mm/yr [Abdrakhmatov *et al.*, 1996; Molnar and Ghose, 2000; Reigber *et al.*, 2001]. The northward motion of the Tien Shan relative to the Eurasia plate varies from ~15 mm/yr in the southern Tien Shan to ~4 mm/yr in the northern part (Figure 1).

[3] Deformation at deep levels beneath the Tien Shan can be investigated by seismic anisotropy studies. Seismic anisotropy is largely a result of lattice preferred orientation of anisotropic minerals, such as olivine and orthopyroxene in the upper mantle. It could reflect deformation in the lithosphere or mantle flow direction in the asthenosphere.

Previous studies of shear-wave splitting in the Tien Shan revealed that the majority of fast orientations are parallel to the strike of the Tien Shan [Makeyeva *et al.*, 1992; Wolfe and Vernon, 1998; Roecker, 2001]. Roecker [2001] published preliminary shear-wave splitting results at 12 of the 28 GHENGIS stations. He found that anisotropy with near EW fast axes at 9 stations and anisotropy at the other 3 stations is not well constrained. Fast orientations in NS are observed in the Issyk Kul area and have been explained as a result of plume-related or small-scale convection in the upper mantle [Makeyeva *et al.*, 1992; Wolfe and Vernon, 1998]. Vinnik *et al.* [2002] modeled receiver functions at several stations in the Tien Shan and found that anisotropy varies significantly with depth.

[4] In this study, we analyzed shear-wave splitting at 30 seismic stations in the Tien Shan, Tarim Basin, and Kazakh platform. Our results provide constraints on seismic anisotropy at a larger number of stations and over a broader region than previous studies in the Tien Shan [Wolfe and Vernon, 1998; Roecker, 2001; Vinnik *et al.*, 2002]. We combine our observations with previous shear-wave-splitting results to reevaluate the mechanism of anisotropy in the Tien Shan and assess the depth extent of the Talasso-Fergana fault.

2. Data and Method

[5] Data used in this study are primarily from the GHENGIS network, a seismic array in the central Tien Shan, northern Tarim Basin, and the Kazakh platform (Figure 1). The GHENGIS network consisted of 28 broadband seismic stations and operated from October 1997 to August 2000. Each station was equipped with a three-component broadband sensor, CMG-3ESP or STS-2. More details about the GHENGIS network can be found in the paper by Roecker [2001], who organized and conducted the experiment. Data at two GEOSCOPE stations, WUS and TLG (squares in Figure 1), are also analyzed.

[6] We have processed data from 36 events whose epicentral distances range from 90° to 125° with mb ≥ 6.0. Only about half of the events (Table 1) have clear SKS signals and give reasonably constrained shear-wave splitting measurements. All the events are from the Tonga Islands and their backazimuths fall in a narrow range from 97° to 106° (Figure 1). This limitation makes it impossible to investigate the variation of shear-wave splitting with event azimuth, which could provide clues on multi-layered anisotropy.

[7] We adopted the method of Silver and Chan [1991] in calculating shear-wave splitting parameters, fast orientation (ϕ) and delay time (δt). The most optimum solution of (ϕ , δt) is obtained by searching a grid of ϕ values from -90° to 90° and a grid of δt values from 0 to 8 s. The errors of splitting

¹Department of Geosciences, University of Houston, Houston, Texas, USA.

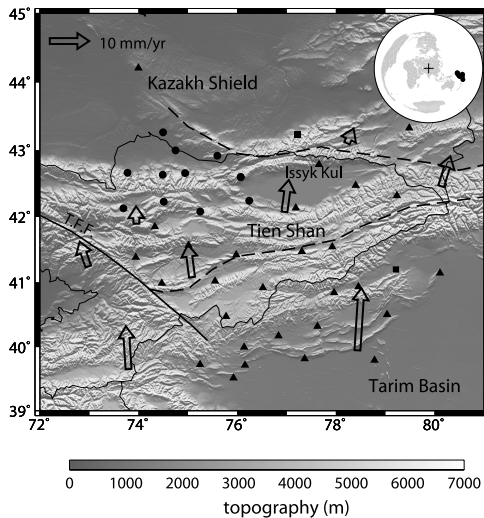


Figure 1. Topography and seismic stations in the central Tien Shan and its vicinity. Triangles are the GHENGIS stations. Circles are stations belonging to the Kazakhstan Network (KNET) and squares are the GEOSCOPE stations. (inset, upper right) Distribution of used events. Abbreviation T.F.F. is for the Talasso-Fergana fault. Dashed lines mark two old sutures. Arrows are surface velocity relative to the Eurasia based on GPS measurements (<http://geoweb.mit.edu/~tah/CAsia/>).

parameters for each individual measurement are estimated using the approach of *Fischer and Yang* [1994].

[8] Both SKS and SKKS phases were analyzed for shear-wave splitting. Because most SKKS phases have poor signal/noise ratios, the results in this paper are only from SKS splitting. An example of SKS waveforms and shear-wave splitting measurements is presented in Figure 2 at two stations, KARL and KOPG, for event 19990917. At the two stations SKS phases are clear on the radial component but are significantly different on the transverse component. A strong phase appears at station KARL while a noise-level signal is recorded at station KOPG. Shear-wave splitting parameters at station KARL are well constrained and show a N64°E fast orientation. At station KOPG, the splitting measurement is a null. Null measurements are generally determined based on the grid search results, in which the obtained delay time is often large (>5s) and the contour is not closed around the optimum point (Figure 2, bottom right). The nulls are further confirmed by the waveform, which shows no SKS energy on the transverse component.

[9] The final splitting parameters and their two standard deviations at one station are obtained as straight weighted means of all non-null measurements. The weighting factor for the i th individual measurement is calculated as $w_i = \min(w_i^\theta, w_i^t) \times w_i^\theta$, where w_i^θ and w_i^t are the weights for fast orientation and delay time, respectively. w_i^θ is a weighting factor based on θ , the difference between the fast direction and the event backazimuth. We assigned w_i^θ as 0.4, 0.6, 0.8, and 1 when θ is <3°, from 3° to 6°, from 6° to 9°, and >9°, respectively. The assumption for w_i^t is that splitting measurements tend to be less well con-

strained when the fast orientation is very close to the event backazimuth.

3. Results

[10] Both fast directions and delay times change significantly across the central Tien Shan (Figure 3 and Table 2). The fast orientations vary from near EW to almost NS and the delay times range from 0.3 s to 2.9 s. Null measurements are observed at 4 stations at the southern Tien Shan front. Despite the diversity in the measurements, anisotropy at nearby stations shows great consistency. (1) Fast orientations at most stations within the Tien Shan range (ARA, KAZ, KAI, DGE, NRN, POG, KARL, CHAT, AHQI, and KENS) are ENE-WSW, roughly parallel to the mountain strike. (2) NNE-SSW fast axes are observed in the western part of the southern Tien Shan and around the Issyk Kul (KASH, TGMT, HARA, KDJ, KAR, and ANA). (3) Azimuthal anisotropy is not detected at stations near the boundary between the southern Tien Shan and the Tarim Basin (XIKR, PIQG, KOPG, and HLQI).

[11] A weighted average of splitting parameters is more reliable if it is calculated from a larger number of individual measurements. For example, at stations ANA, KAR, KAZ, KENS, KHA, KSA, NRN, PDG, WQIA, and WUS, the results are well constrained since at least 3 individual measurements are used in calculating the averages. The delay times at these stations vary from 1.1 s to 1.7 s, compatible with delay times worldwide [*Silver*, 1996]. Large delay times of 1.9 s to 2.9 s appear at several stations (AHQI, CHAT, DGE, HARA, KDJ, and TGMT), where there are only 1 or 2 individual measurements. Two standard deviations on these delay times are from 0.5 to 0.7s, much larger than those (0.2–0.3 s) at stations where there are more individual measurements. The large delay times are therefore likely due to large uncertainties rather than strong anisotropy.

4. Discussion and Conclusions

[12] The strike-parallel (ENE-WSW) fast orientations determined in this study are consistent with previous shear-wave splitting results in the central and western Tien Shan [*Makeyeva et al.*, 1992; *Wolfe and Vernon*, 1998; *Roecker*, 2001; *Vinnik et al.*, 2002]. Such strike-parallel

Table 1. Earthquakes Used in This Study

yyyymmdd	Latitude, °	Longitude, °	Depth, km	Mb	Δ , °	Baz, °
20000815	-31.56	179.74	350	6.8	120	107
20000803	-12.13	166.42	73	6.5	98	99
20000614	-25.63	178.06	631	7.0	115	102
19991229	-10.95	165.39	33	6.4	97	99
19991126	-16.32	168.13	35	7.1	102	101
19990918	-19.74	169.21	117	6.1	105	103
19990917	-13.81	167.22	212	6.3	100	100
19990822	-16.05	168.02	29	6.2	102	101
19990718	-22.48	179.44	565	6.8	114	99
19990525	-19.14	169.38	263	6.4	105	102
19990409	-26.38	178.22	625	6.4	116	103
19990206	-12.89	166.68	111	7.2	99	99
19981114	-14.97	167.34	129	6.0	101	100
19980921	-13.63	166.79	55	6.5	100	100
19980716	-11.09	166.17	110	6.4	97	98
19980104	-22.23	170.9	76	6.7	108	104
19971115	-15.13	167.34	129	6.3	101	101

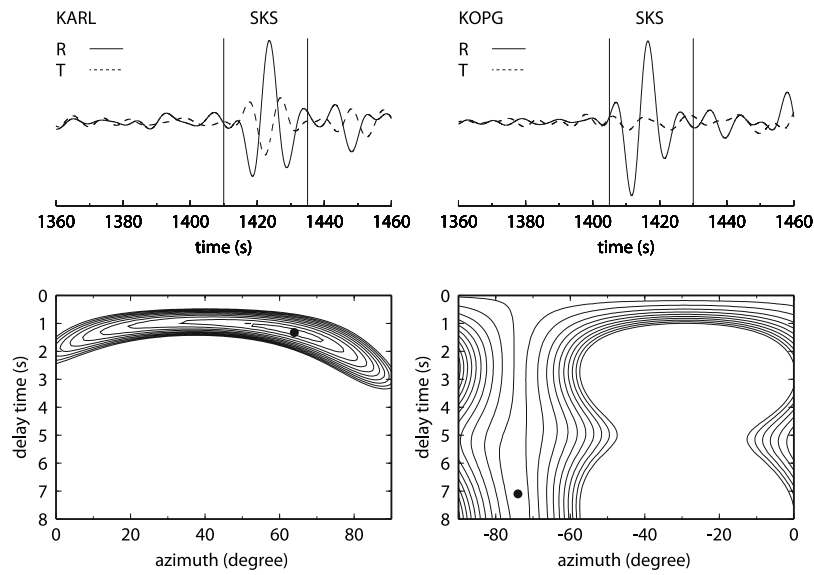


Figure 2. Seismograms of SKS phases and the splitting measurements at two stations for the event 19990917 (Table 1). (left) Station KARL; (right) Station KOPG. Radial component and transverse component are indicated by solid and dashed lines, respectively. Shear-wave splitting parameters are well constrained at KARL and a null is observed at KOPG.

anisotropy is typical in continental mountain belts [Silver and Chan, 1991; Silver, 1996] since the maximum strain tends to align with the direction of the minimum stress, which is perpendicular to the collision direction.

[13] Three candidates may contribute to the observed strike-parallel anisotropy. They are crustal anisotropy, coherent deformation in the mantle lithosphere, and strike-

parallel asthenospheric flow. Crustal anisotropy is often considered small and negligible. This might not be appropriate in continental orogenies, where crust is usually thick, for example, 50–65 km in the central Tien Shan [Vinnik et al., 2004]. Receiver function analyses by Vinnik et al. [2002] show 2–6% anisotropy in the crust at several stations in the Tien Shan. It is likely that the mantle

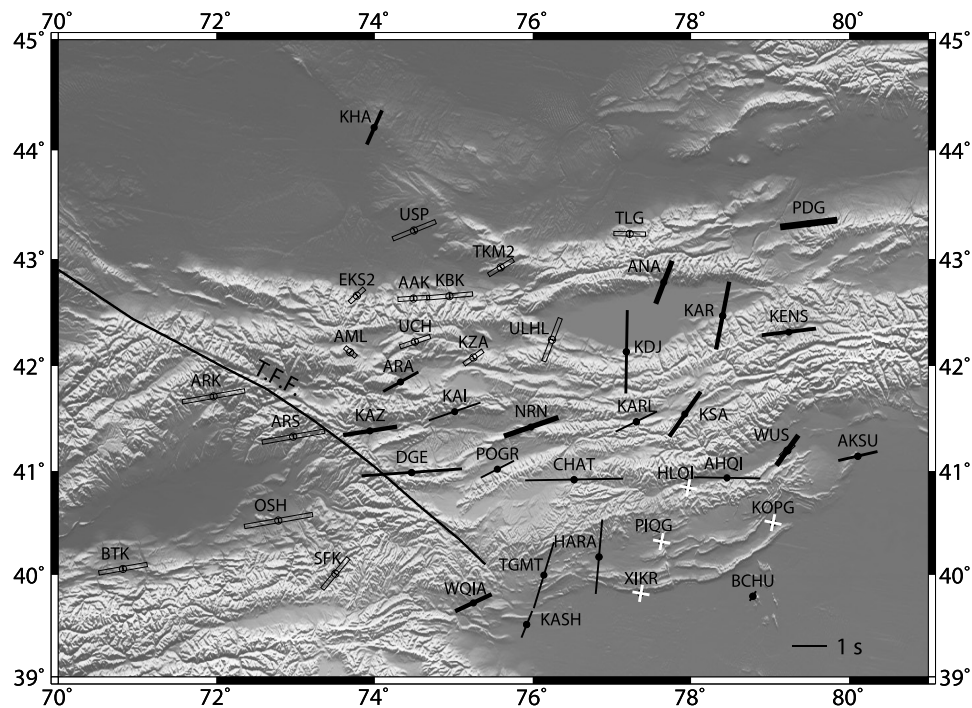


Figure 3. Shear-wave splitting measurements from this study (solid bars) and from previous studies (open bars) [Makeyeva et al., 1992; Wolfe and Vernon, 1998]. The orientation of a bar indicates fast orientations and the bar length is proportional to delay times. The width of a solid bar is proportional to the number of individual measurements at a station. Null measurements are plotted as white crosses. The two lines of a cross are oriented parallel and orthogonal to the event backazimuth direction, respectively.

Table 2. Shear-Wave Splitting Results

Station	Longitude, °	Latitude, °	ϕ , °	δt , s	Number
AHQI	78.46	40.93	-89 ± 7	1.9 ± 0.5	1
AKSU	80.11	41.14	77 ± 9	1.2 ± 0.4	2
ANA	77.66	42.78	21 ± 8	1.3 ± 0.3	5
ARA	74.33	41.85	61 ± 7	1.2 ± 0.2	2
BCHU	78.78	39.79	33 ± 19	0.3 ± 0.2	1
CHAT	76.52	40.92	89 ± 2	2.8 ± 0.6	1
DGE	74.47	40.99	86 ± 4	2.9 ± 0.6	2
HARA	76.84	40.17	5 ± 2	2.2 ± 0.4	1
KAI	75.01	41.57	71 ± 6	1.6 ± 0.1	1
KAR	78.40	42.47	11 ± 3	2.0 ± 0.5	4
KARL	77.31	41.47	64 ± 6	1.3 ± 0.2	1
KASH	75.92	39.52	22 ± 11	0.8 ± 0.3	1
KAZ	73.94	41.38	81 ± 10	1.6 ± 0.5	4
KDJ	77.19	42.13	1 ± 4	2.4 ± 0.5	2
KENS	79.24	42.32	83 ± 7	1.6 ± 0.3	3
KHA	74.00	44.21	24 ± 10	1.1 ± 0.3	3
KSA	77.93	41.54	35 ± 9	1.6 ± 0.3	4
NRN	75.98	41.42	71 ± 5	1.7 ± 0.2	5
PDG	79.49	43.33	83 ± 5	1.7 ± 0.3	7
POGR	75.55	41.02	63 ± 15	1.1 ± 0.3	1
TGMT	76.14	40.00	17 ± 9	2.0 ± 0.7	1
WQIA	75.25	39.73	65 ± 5	1.2 ± 0.2	4
WUS	79.22	41.20	36 ± 9	1.1 ± 0.3	5

lithosphere of the central Tien Shan deforms coherently with the crust as its lower crust is not seismically slow and presumably strong [Vinnik *et al.*, 2004]. This is different from southern Tibet where it is proposed that a slow mid-lower crust causes decoupling between the crust and the mantle [Royden *et al.*, 1997; Yao *et al.*, 2006]. The coherent lithosphere deformation in the Tien Shan helps to align olivine *a* axes in the direction of the mountain belts and produce the observed strike-parallel fast orientations. In addition, there could be strike-parallel asthenospheric flow beneath the central Tien Shan, which also contributes to the observed anisotropy. Teleseismic SKS phases alone in this study cannot single out the source of anisotropy beneath the central Tien Shan. Other methods such as receiver function analyses and surface wave studies would provide better estimates on the depth distribution of anisotropy.

[14] The NNE-SSW fast orientations require a different explanation than those observed within the deformed Tien Shan range. This type of anisotropy was first observed around the Issyk Kul by Makeyeva *et al.* [1992], who hypothesized that such anisotropy was caused by mantle convection related to a plume beneath the area. Analyzing shear-wave splitting at the KNET stations, Wolfe and Vernon [1998] found that the mantle plume mechanism was unable to explain the overall pattern of anisotropy and preferred a more general small-scale convection model. In this study, we observed NNE-SSW fast orientations in the Issyk Kul area and in the western part of the southern Tien Shan, ~ 200 km south to the Issyk Kul. The consistency in the fast orientation at these two areas is in contrast to the predictions of the small-scale convection model, and thus suggests a common and regional-scale cause. The NNE-SSW direction coincides with the surface motion in the central Tien Shan according to GPS measurements [Abdrakhmatov *et al.*, 1996]. We hypothesize that these fast orientations are produced by shear between the northward moving lithosphere and underlying asthenosphere. The lithospheric component of anisotropy is probably small in

both areas where the lithosphere is likely strong and less deformed.

[15] Although the null measurements in this study are the first to be reported in the Tien Shan region, the lack of azimuthal anisotropy has been observed in other continental collision fronts, such as in Himalayas and southern Tibet [Sandvol *et al.*, 1994, 1997; Chen and Ozalaybey, 1998; Huang *et al.*, 2000]. There are several ways to interpret the nulls in the Tien Shan. One simple explanation is that they reflect azimuthally isotropic structure beneath the southern Tien Shan. This seems unlikely as nearby stations show obvious splitting of SKS phases. Another possible interpretation of the nulls is that these stations are near the boundary of two different types of anisotropic media. Our results show that the nulls are obtained in between regions that display NNE-SSW fast orientations and ENE-WSW fast orientations. The other possibility is that the local anisotropy has a fast axis in NNE-SSW, similar to those at nearby stations (HARA, TGMT, and KASH). In this case, shear-wave splitting cannot be detected since the fast orientation is orthogonal to the event backazimuths (95° – 105°). Therefore, the nulls would have a similar origin as anisotropy with NNE-SSW fast axes, which we attribute to shear between the lithosphere and asthenosphere.

[16] Although the Talasso-Fergana fault marks a clear transition of upper mantle properties from the western to the central Tien Shan [Kosarev *et al.*, 1993; Roecker *et al.*, 1993], it seems to have little effect on local anisotropy. Fast orientations at stations near the Talasso-Fergana fault (ARK, ARS, KAZ, and DGE) are more EW, which are consistent with the anisotropy away from the fault in the Tien Shan, but different from the NW-SE strike of the fault. This observation is in contrast to those in Tibet where anisotropy near major transform faults, such as the Kunlun fault and the Altyn Tagh fault, tend to be oriented sub-parallel to the fault strike [Guilbert *et al.*, 1996; Herquel *et al.*, 1999]. The correlation of anisotropy with strike-slip faults in Tibet indicates that these faults extend through the lithosphere [Lave *et al.*, 1996]. The active slip rate along the Talasso-Fergana fault is 8–16 mm/yr [Burtman *et al.*, 1996], which is similar to the slip rate of ~ 9 mm/yr along the Altyn Tagh fault [Shen *et al.*, 2001]. Given that the Talasso-Fergana fault actively accommodates significant deformation in the region, the lack of correlation between anisotropy and the fault strike suggests that the fault must be shallow and is probably confined to the crust.

[17] **Acknowledgments.** We thank Steven Roecker for providing some references and thank Tom Herring for making the GPS measurements online. Comments from Michael Murphy, Martha Savage, and one anonymous reviewer helped to improve this paper. Seismic data are obtained through the IRIS/DMC. Figures are produced using the GMT software [Wessel and Smith, 1998]. This work is supported by NSF grant EAR0536948.

References

- Abdrakhmatov, K. Y., *et al.* (1996), Relative recent construction of the Tien Shan inferred from GPS measurements of present day crustal deformation rates, *Nature*, 384, 450–453.
- Burtman, V. S., S. F. Skobelev, and P. Molnar (1996), Late Cenozoic slip on the Talas-Ferghana fault, the Tien Shan, central Asia, *Geol. Soc. Am. Bull.*, 108, 1004–1021.
- Chen, W.-P., and S. Ozalaybey (1998), Correlation between seismic anisotropy and Bouguer gravity anomalies in Tibet and its implications for lithospheric structures, *Geophys. J. Int.*, 135, 93–101.

- Fischer, K. M., and X. Yang (1994), Anisotropy in Kuril-Kamchatka subduction zone structure, *Geophys. Res. Lett.*, *21*, 5–8.
- Guilbert, J., G. Poupinet, and M. Jiang (1996), A study of azimuthal P residuals and shear-wave splitting across the Kunlun range (northern Tibet plateau), *Phys. Earth. Planet. Inter.*, *95*, 167–174.
- Herquel, G., P. Tapponnier, G. Wittlinger, M. Jiang, and D. Shi (1999), Teleseismic shear wave splitting and lithospheric anisotropy beneath and across the Altyn Tagh fault, *Geophys. Res. Lett.*, *26*, 3225–3228.
- Huang, W., et al. (2000), Seismic polarization anisotropy beneath the central Tibet Plateau, *J. Geophys. Res.*, *105*, 27,979–27,989.
- Kosarev, G. L., N. V. Petersen, L. P. Vinnik, and S. W. Roecker (1993), Receiver functions for the Tien Shan analog broadband network: Contrasts in the evolution of structure across the Talasso-Fergana Fault, *J. Geophys. Res.*, *98*, 4437–4448.
- Lave, J., J. P. Avouac, R. Lacassin, P. Tapponnier, and J. P. Montagner (1996), Seismic anisotropy beneath Tibet: Evidence for eastward extrusion of the Tibetan lithosphere?, *Earth Planet. Sci. Lett.*, *140*, 83–96.
- Makeyeva, L. I., L. P. Vinnik, and S. W. Roecker (1992), Shear-wave splitting and small-scale convection in the continental upper mantle, *Nature*, *358*, 144–147.
- Molnar, P., and S. Ghose (2000), Seismic moments of major earthquakes and the rate of shortening across the Tien Shan, *Geophys. Res. Lett.*, *27*, 2377–2380.
- Reigber, C. H., et al. (2001), New space geodetic constraints on the distribution of deformation in Central Asia, *Earth Planet. Sci. Lett.*, *191*, 157–165.
- Roecker, S. W. (2001), Constraints on the crust and upper mantle of the Kyrgyz Tien Shan from the preliminary analysis of CHENGIS broadband data, *Russ. Geol. Geophys.*, *42*, 1554–1565.
- Roecker, S. W., T. M. Sabitova, L. P. Vinnik, Y. A. Burmakov, M. I. Golvanov, R. Mamatkanova, and L. Munirova (1993), Three-dimensional elastic wave velocity structure of the western and central Tien Shan, *J. Geophys. Res.*, *98*, 15,779–15,795.
- Royden, L., B. C. Burchfiel, R. W. King, E. Wang, Z. Chen, F. Shen, and Y. Liu (1997), Surface deformation and lower crust flow in eastern Tibet, *Science*, *276*, 788–790.
- Sandvol, E., J. Ni, and T. M. Hearn (1994), Seismic azimuthal anisotropy beneath the Pakistan Himalayas, *Geophys. Res. Lett.*, *21*, 1635–1638.
- Sandvol, E., J. Ni, R. Kind, and W. Zhao (1997), Seismic anisotropy beneath the southern Himalayas-Tibet collision zone, *J. Geophys. Res.*, *102*, 17,813–17,823.
- Shen, Z. K., M. Wang, Y. Li, D. D. Jackson, A. Yin, D. Dong, and P. Feng (2001), Crustal deformation along the Altyn Tagh fault system, western China, from GPS, *Geophys. Res. Lett.*, *106*, 30,607–30,621.
- Silver, P. G. (1996), Seismic anisotropy beneath the continents: Probing the depth of geology, *Annu. Rev. Earth Planet. Sci.*, *24*, 385–432.
- Silver, P. G., and W. W. Chan (1991), Shear-wave splitting and subcontinental mantle deformation, *J. Geophys. Res.*, *96*, 16,429–16,454.
- Vinnik, L., D. Peregoudov, L. Makeyeva, S. Oreshin, and S. Roecker (2002), Towards 3-D fabric in the continental lithosphere and asthenosphere: The Tien Shan, *Geophys. Res. Lett.*, *29*(16), 1791, doi:10.1029/2001GL014588.
- Vinnik, L. P., et al. (2004), Receiver function tomography of the central Tien Shan, *Earth Planet. Sci. Lett.*, *225*, 131–146.
- Wessel, P., and W. H. F. Smith (1998), New improved version of the generic mapping tools released, *EOS Trans. AGU*, *79*(47), 579.
- Windley, B. F., M. B. Allen, C. Zhang, Z. Zhao, and G. Wang (1990), Paleozoic accretion and Cenozoic reformation of the Chinese Tien Shan Range, central Asia, *Geology*, *18*, 128–131.
- Wolfe, C. J., and F. L. Vernon III (1998), Shear-wave splitting at central Tien Shan: evidence for rapid variation of anisotropic patterns, *Geophys. Res. Lett.*, *25*, 1217–1220.
- Yao, H., R. D. Van der Hilst, and M. V. De Hoop (2006), Surface-wave array tomography in SE Tibet from ambient seismic noise and two-station analysis: I. Phase velocity maps, *Geophys. J. Int.*, *166*, 732–744.
- Yin, A., S. Nie, P. Craig, T. M. Harrison, F. J. Ryerson, X. Qian, and G. Yang (1998), Late Cenozoic tectonic evolution of the southern Chinese Tien Shan, *Tectonics*, *17*, 1–27.

C. Chen and A. Li, Department of Geosciences, University of Houston, 4800 Calhoun Road, Houston, TX 77004, USA. (ali2@mail.uh.edu)